

# Facile Synthesis of Multimeric Micelles\*\*

Ung Yeol Lee, Nam Muk Oh, Dong Sup Kwag, Kyung Taek Oh, Young Taik Oh, Yu Seok Youn, and Eun Seong Lee\*

There has been a growing interest in the development of colloidal micelles that can offer various applications in the biomedical or cosmetic fields.<sup>[1–7]</sup> These micelles can potentially function as carriers for biological species, diagnostic agents, and other biorelated devices.<sup>[1–7]</sup> Among these, the use of micelles for the transport of biological species is particularly exciting, with potentially significant applications in pharmaceuticals or cosmetics.<sup>[4–7]</sup> Much research has focused on developing nanoplateforms for biological species, usually adopting functional amphiphilic polymers for constituting a micellar core or corona.<sup>[1–7]</sup> The unique properties of these micelles allow a precise control of the release of the encapsulated species.<sup>[4–7]</sup> However, the one-core and one-shell architecture of the micelle remains unchanged, often impeding precise control of release for the multiple species encapsulated in the micelle.<sup>[8]</sup> Generation of a multi-compartment micelle, evolved from the di-compartment (core/shell) morphology, can be a means to building a micelle-to-micelle architecture containing a link between different micelles. This morphology can enable tailored control of release for various biological species entrapped in the compartments, expanding the application of micelles into diverse fields of science and technology. In this study, we developed a micelle-to-micelle fabrication using monofunctionalized micelles to prepare flexible dimeric, trimeric, tetrameric, multimeric micelles, as well as a more complex micellar cluster. This technique utilizes two-armed, three-armed, four-armed junctions, and

multiple junctions to link micelles. This newly proposed architecture may be more useful than any micelle fabrication developed thus far.<sup>[1–9]</sup>

Scheme 1 and Figure 1 show the precursor substrate (SiO<sub>2</sub> particle) and its use in the preparation of multimeric micelles. The surface amino groups of functionalized SiO<sub>2</sub> particles were modified with dimethylmaleic anhydride (DMA),<sup>[10,11]</sup> high-molecular weight poly(ethylene glycol) (hPEG,  $M_w$  = 10 kDa), cystamine, and biocompatible poly(L-lactic acid)-*b*-poly(ethylene glycol) (PLLA-*b*-PEG;  $M_w$  = 1 kDa and 2 kDa, respectively)<sup>[12]</sup> at room temperature (Scheme 1). Briefly, dimethylmaleic acid groups were added to the free amino groups of functionalized SiO<sub>2</sub> particles using DMA, and the residual amino groups were treated with succinylated hPEG (hPEG-NHS), in the presence of triethylamine (TEA, as a catalyst) in dimethylsulfoxide (DMSO). hPEG was used to improve the colloidal stability of SiO<sub>2</sub> particles in aqueous solution. Dimethylmaleic acid groups of the functionalized SiO<sub>2</sub> particles were pre-activated using *N,N'*-dicyclohexylcarbodiimide (DCC) and *N*-hydroxysuccinimide (NHS),<sup>[12]</sup> and were treated with excess cystamine. After cleaning the SiO<sub>2</sub> particles with fresh DMSO, succinylated PLLA-*b*-PEG (PLLA-*b*-PEG-NHS) was coupled to cystamine-group of the SiO<sub>2</sub> particles, generating a disulfide linkage between the SiO<sub>2</sub> particles and the PLLA-*b*-PEG (Scheme 1, Figure 1a).

When fresh amphiphilic polymers are added, they self-assemble<sup>[1–7]</sup> (Figure 1b) around PLLA-*b*-PEG conjugated to SiO<sub>2</sub> particles in an aqueous solution; this assembly led to the formation of micelles fixed to the SiO<sub>2</sub> particle. A field-emission scanning emission microscope (FE-SEM) image shows micelles clinging to the surface of a SiO<sub>2</sub> particle (Figure 1c). After the chemical linkage (i.e. disulfide bond) between the SiO<sub>2</sub> particle and the micelle has been cleaved using a reducing agent (dithiothreitol, DTT),<sup>[13,14]</sup> monothiol-functionalized micelles were released. Our fluorescent analysis reveals that there were an average of  $0.96 \pm 0.13$  thiol groups per micelle (Supplementary Information). The hPEG blocks linked to SiO<sub>2</sub> particles are located between the growing micelles, which might help minimize intermicellar interactions, resulting in monothiol-functionalized micelles. FE-SEM images show the spherical shape of one monothiol-functionalized micelle separated from the SiO<sub>2</sub> particle and the cleaned SiO<sub>2</sub> particle (without micelles) following cleavage with DTT (Figure 1d).

Figure 2a illustrates the direct coupling between two micelles to form a dimeric micelle. A monothiol-functionalized micelle (approximately 80 nm diameter) was pre-activated with excess functionalized PEG (PEG with two maleimide (Mal) groups, Mal-PEG-Mal,  $M_w$  = 2 kDa) to produce a monoMal-functionalized micelle, and was coupled

[\*] U. Y. Lee, N. M. Oh, D. S. Kwag, Prof. Dr. E. S. Lee  
Division of Biotechnology, The Catholic University of Korea  
43-1 Yeokgok 2-dong, Wonmi-gu, Bucheon, Gyeonggi-do 420-743  
(Republic of Korea)  
E-mail: eslee@catholic.ac.kr

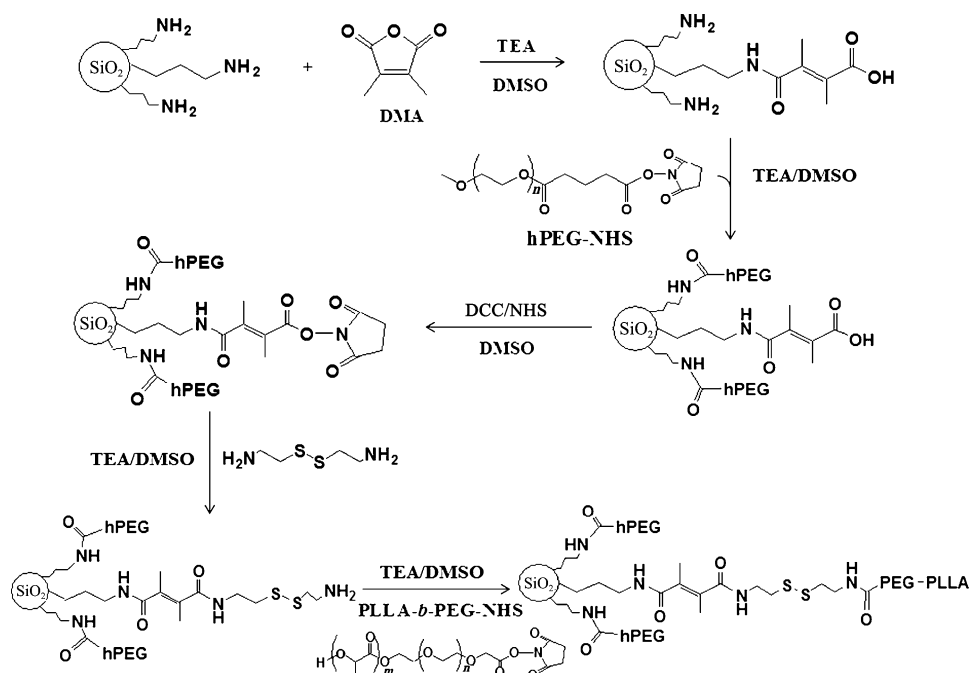
Prof. Dr. K. T. Oh  
College of Pharmacy, Chung-Ang University  
Seoul 155-756 (Republic of Korea)

Prof. Dr. Y. T. Oh  
Department of Diagnostic Radiology  
Yonsei University College of Medicine  
Seoul 120-752 (Republic of Korea)

Prof. Dr. Y. S. Youn  
College of Pharmacy, Sungkyunkwan University  
Suwon 440-726 (Republic of Korea)

[\*\*] This work was financially supported by the Basic Science Research Program through the National Research Foundation of Korea (NRF) funded by the Ministry of Education, Science, and Technology (No. 2010-0007126), and by the Gyeonggi Regional Research Center (GRRC).

Supporting information for this article (descriptions of and data regarding the synthesis of multimeric micelles and other experimental procedures) is available on the WWW under <http://dx.doi.org/10.1002/anie.201202190>.

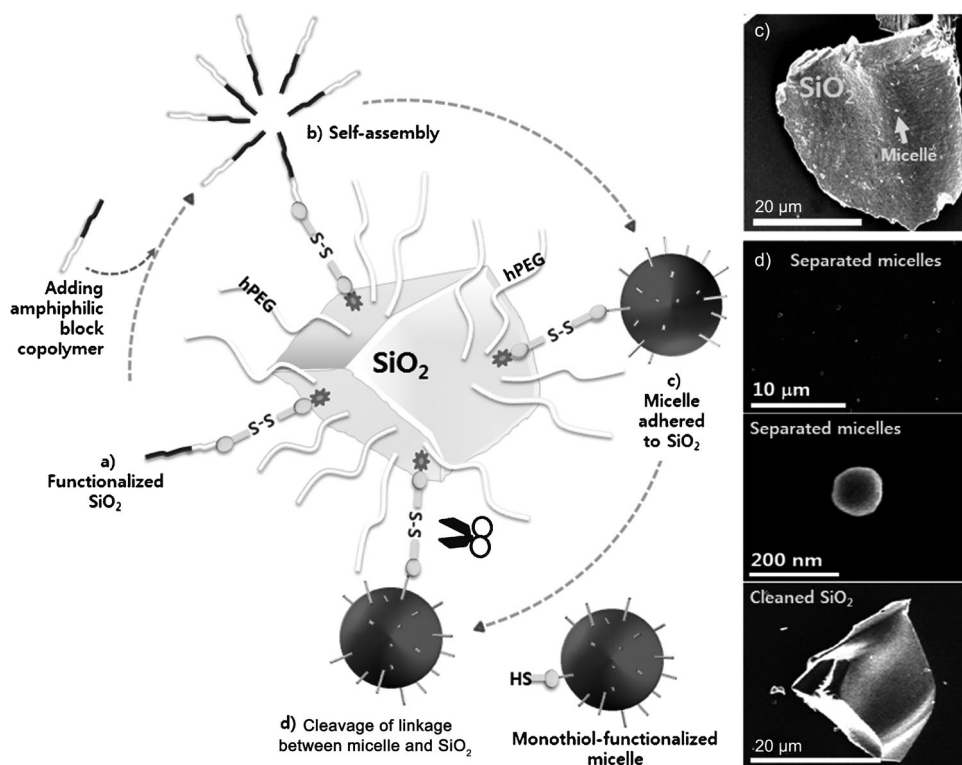


**Scheme 1.** Functionalization of  $\text{SiO}_2$  particles. See text for details.

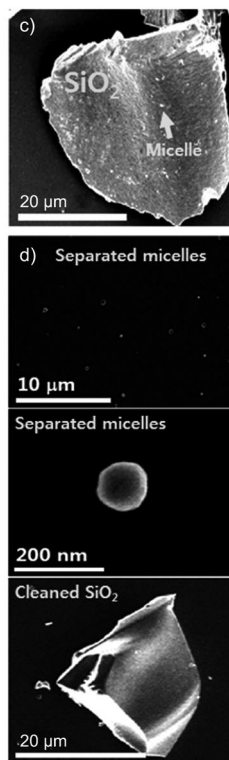
with the other monothiol-functionalized micelle by a simple reaction between the maleimide group and the thiol group. According to the atomic force microscope (AFM) image, the

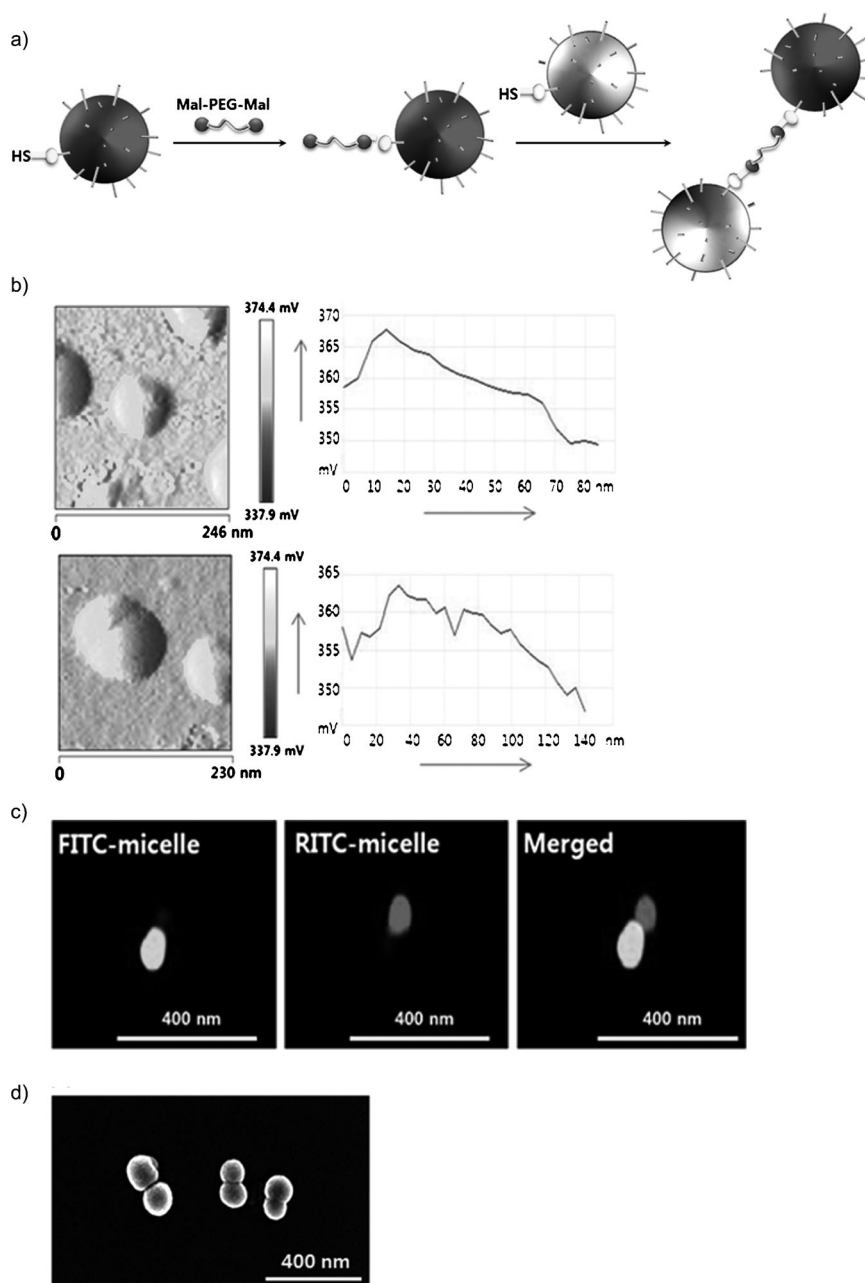
the selective encapsulation of biological species within each compartment (Figure 2c) can mediate distinct spatial transport of bioactive species. This is an example of how nano-structured micelle aggregates can be arranged and their unique properties harnessed using simple conjugation chemistry between the micelles.

Figure 3a shows a simple coupling procedure between two monothiol-functionalized micelles. We utilized dimethylsulfoxide (DMSO)-mediated oxidation<sup>[15]</sup> of thiol groups to generate a disulfide linkage between the monothiol-functionalized micelles, generating dimeric micelles. At 25°C, dimeric micelle synthesis was slightly improved with increasing DMSO exposure time, as estimated from the linear regression of  $\log(\% \text{DMSO} + 1)$  versus the percent of dimeric micelles (Figure 3b,c). This dimeric micelle generation also increased with temperature (0–40°C), but at 70°C extensive coagulation between micelles occurred from the dehydration of the micellar hydrophilic corona upon heating.<sup>[7]</sup> The fraction of total



**Figure 1.** Schematic drawing of the synthesis of a monofunctionalized micelle from a) a functionalized  $\text{SiO}_2$  particle (see Scheme 1). b) Site-specific self-assembly process of amphiphilic polymers on the surface of the functionalized  $\text{SiO}_2$  particle allows c) the fabrication of a micelle bound to the  $\text{SiO}_2$  particle (FE-SEM image). d) FE-SEM images of the micelles or  $\text{SiO}_2$  particle after using DTT to cleave the disulfide linkage between the  $\text{SiO}_2$  particle and the micelle.





**Figure 2.** Schematic drawing of the synthesis of a) a Janus-like dimeric micelle. See the text for more details. b) AFM images of monothiol-functionalized micelles (top) or Janus-like dimeric micelles (bottom). c) Fluorescent images or d) FE-SEM image of Janus-like dimeric micelles.

micelles in dimeric form ( $F_{di}$ ) reached a maximum of 80 % at 40 °C. This controlled formation of dimeric micelles is a unique feature of our technique. In addition, to confirm that the disulfide bond formation between micelles is what causes the dimeric micelle formation, dimeric micelles prepared in DMSO (20 wt %) at 40 °C were treated with reductive DTT (100 mM) in PBS (pH 7.4) at room temperature for 2 h. Dimeric micelles were completely cleaved into single micelles (Supporting Information, Figure S1), which indicates that dimeric micelles were initially formed through disulfide bond formation.

Another remarkable feature is that the bonds between the micelles can be customized, providing considerable opportunity for additional colloidal applications. As shown in Figure 4, we extended the micelle-to-micelle binding to prepare multimeric micelles, these formed according to the binding angles between the micelles. We utilized 1,1,1-tri(hydroxymethyl)propane (TMOP), four-armed carboxymethyl PEG ( $M_w = 10$  kDa), and bovine serum albumin (BSA) to link the micelles.

First, the hydroxy groups of TMOP (three-arm structure) were modified in dimethylformamide (DMF) using succinyl anhydride, 4-dimethylaminopyridine (DMAP), and TEA, to prepare carboxylated TMOP (Supporting Information, Figure S2). The carboxylated TMOP collected after recrystallization using DMF and excess diethyl ether was pre-activated in DMF using DCC and NHS, and was treated with *N*-(2-aminoethyl)maleimide (AEM)<sup>[6]</sup> at room temperature (Supporting Information, Figure S2). Maleimide-linked TMOP (TMOP-Mal) was coupled to three monothiol-functionalized micelles in a  $\text{Na}_2\text{B}_4\text{O}_7$  buffer solution (0.1 mM, pH 7.4). As a result, the trimeric micelle (tightly jointed between the micelles) was the primary product over the dimeric micelle, which formed as a byproduct (Figure 4a):  $F_{di} = 14 \pm 5\%$ , the fraction of trimeric micelles ( $F_{tri}$ ) =  $78 \pm 7\%$ . In addition, a detailed FE-SEM image reveals that the steric strain of each micelle on the trimeric micelle caused a micellar fusion at the contact area of the micelles.

Second, to overcome the steric hindrance and intermicellar strain that may be present between four binding micelles, we selected a four-armed carboxymethyl PEG that has four long, flexible PEG chains. Before the coupling process with monothiol-functionalized micelles, a four-armed carboxymethyl PEG was pre-activated in dichloromethane using DCC and NHS, and was treated with AEM (Supporting Information, Figure S3). Mal-linked four-armed PEG was then coupled to four monothiol-functionalized micelles in a  $\text{Na}_2\text{B}_4\text{O}_7$  buffer solution (0.1 mM, pH 7.4), resulting in tetrameric micelle formation (Figure 4b). In this preparation, the tetrameric micelles constitute the majority of the micelles produced:  $F_{di} = 10 \pm 4\%$ ,  $F_{tri} = 13 \pm 5\%$ , the fraction of tetrameric micelles ( $F_{tetra}$ ) =  $71 \pm 6\%$ .

Third, to prepare an intermediate host for multiple-binding micelles, BSA ( $M_w$  66.5 kDa), one of the plasma

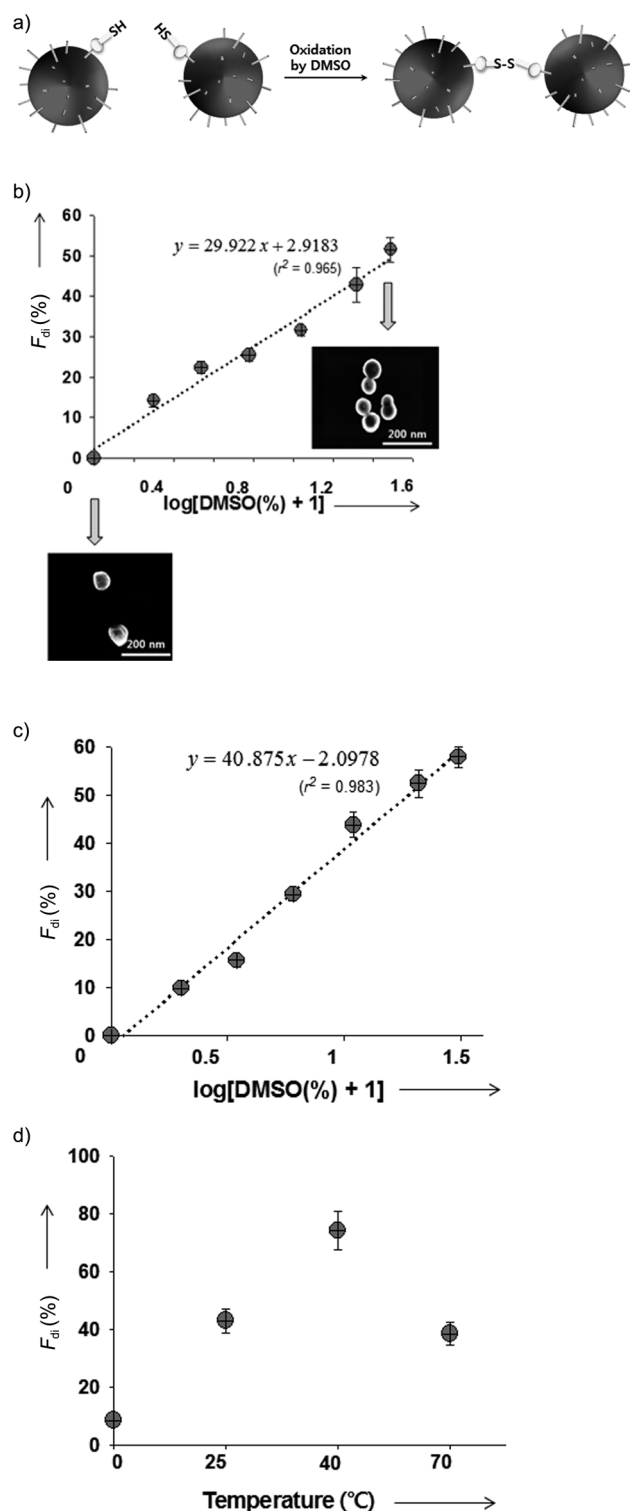


**Figure 3.** DMSO-induced dimeric micelle synthesis: a) micelle coupling scheme. Percent of total micelles in dimeric form ( $F_d$ ) formed from monothiol-functionalized micelles by treatment with DMSO (0–30 wt%) in aqueous solution after b) 4 h or c) 8 h stirring (100 rpm) at 25 °C (average of three experiments,  $n=3$ ). FE-SEM images of micelles are shown in (b). d) Temperature-controlled dimeric micelle formation at 0–70 °C with DMSO (20 wt%) in aqueous solution ( $n=3$ ).

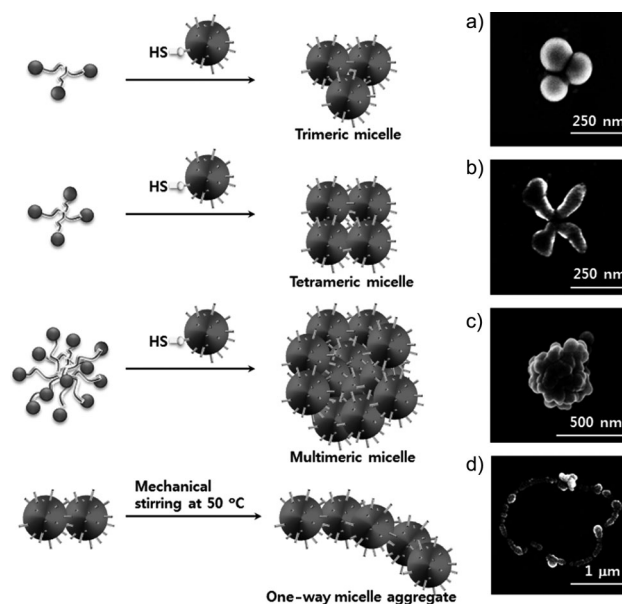


**Figure 4.** Various multimeric-micelles are formed according to the number of micelle-binding junctions: a) three-armed junction, b) four-armed junction, c) multiple junctions, and d) one-way junction.

proteins, was cross-linked<sup>[5]</sup> using ethylenediamine in PBS solution (pH 6.0) in the presence of catalytic 1-ethyl-3-dimethylaminopropylcarbodiimide (EDC) and was treated with AEM. The Mal-linked BSA (BSA-Mal) cluster (approximately 50 nm diameter; Supporting Information, Figure S4) was treated with monothiol-functionalized micelles. As a result, the monothiol-functionalized micelles were bound to the BSA cluster in a racemose manner, forming multimeric micelles (Figure 4c).

Fourth, the dimeric micelle solution was mechanically stirred at 1000 rpm in PBS solution (pH 7.4) at 50 °C for 1 day. With the externally applied mechanical stirring, dimeric micelles were organized into chains, with the help of a lipophilic interaction between the micellar shells. The heating at 50 °C causes dehydration of the micellar shells facilitating the lipophilic interaction.<sup>[7]</sup> This process generated one-way multimeric micelles as shown in Figure 4d, which is similar to the formation of linear aggregates of latex particles in a shear field.<sup>[16]</sup>

Highly precise control of micellar structures has been challenging. The method reported herein can satisfy the need to build novel hybrid micellar blocks for various applications. Taken together, our results demonstrate that control over the binding of colloidal micelles, using monofunctionalized micelles prepared from a SiO<sub>2</sub> precursor substrate, enables a precise micelle-to-micelle assembly. Such fabrication methods produce flexible dimeric, trimeric, tetrameric, and multimeric micelles, as well as a more complex micellar cluster. This strategy can only be applied to amphiphilic block copolymers, which produce micelles with a “frozen-in” micellar core. This micelle-to-micelle fabrication should offer unprecedented opportunities for engineering smart micelles as a future nanosize material.

Received: March 20, 2012  
Revised: April 23, 2012  
Published online: June 13, 2012

**Keywords:** amphiphiles · disulfide linkage · micelles · multimeric micelles · nanoparticles

- [1] J. W. Yoo, D. J. Irvine, D. E. Discher, S. Mitragotri, *Nat. Rev. Drug Discovery* **2011**, *10*, 521–535.
- [2] S. Srivastava, N. A. Kotov, *Soft Matter* **2009**, *5*, 1146–1156.
- [3] R. Chandrawati, M. P. van Koeveden, H. Lomas, F. Caruso, *J. Phys. Chem. Lett.* **2011**, *2*, 2639–2649.
- [4] S. Y. Park, H. J. Baik, Y. T. Oh, K. T. Oh, Y. S. Youn, E. S. Lee, *Angew. Chem.* **2011**, *123*, 1682–1685; *Angew. Chem. Int. Ed.* **2011**, *50*, 1644–1647.
- [5] E. S. Lee, D. Kim, Y. S. Youn, K. T. Oh, Y. H. Bae, *Angew. Chem.* **2008**, *120*, 2452–2455; *Angew. Chem. Int. Ed.* **2008**, *47*, 2418–2421.
- [6] D. J. Pochan, Z. Chen, H. Cui, K. Hales, K. Qi, K. L. Wooley, *Science* **2004**, *306*, 94–97.
- [7] L. M. Walker, *Curr. Opin. Colloid Interface Sci.* **2011**, *16*, 451–456.
- [8] H. Wang, Y. Zhao, Y. Wu, Y. Hu, K. Nan, G. Nie, H. Chen, *Biomaterials* **2011**, *32*, 8281–8290.
- [9] L. Y. Qiu, Y. H. Bae, *Pharm. Res.* **2006**, *23*, 1–30.
- [10] B. R. Lee, K. T. Oh, Y. T. Oh, H. J. Baik, S. Y. Park, Y. S. Youn, E. S. Lee, *Chem. Commun.* **2011**, *47*, 3852–3854.
- [11] N. M. Oh, D. S. Kwag, K. T. Oh, Y. S. Youn, E. S. Lee, *Biomaterials* **2012**, *33*, 1884–1893.
- [12] W. R. Lee, K. T. Oh, S. Y. Park, N. Y. Yoo, Y. S. Ahn, D. H. Lee, Y. S. Youn, D. K. Lee, K. H. Cha, E. S. Lee, *Colloids Surf. B* **2011**, *85*, 379–384.
- [13] H. Mok, S. H. Lee, J. W. Park, T. G. Park, *Nat. Mater.* **2010**, *9*, 272–278.
- [14] S. Y. Park, K. T. Oh, Y. T. Oh, N. M. Oh, Y. S. Youn, E. S. Lee, *Chem. Commun.* **2012**, *48*, 2522–2524.
- [15] W. W. Epstein, F. W. Sweat, *Chem. Rev.* **1967**, *67*, 247–260.
- [16] P. A. Reynolds, *Colloids Surf.* **1984**, *11*, 145–154.